RSC Advances

ROYAL SOCIETY OF CHEMISTRY

www.rsc.org/advances

Application of Magnetite Nano-hybrid Epoxy As Protective Marine Coatings for Steel

Ayman M. Atta,*[a,b] [c]*Ashraf M. El-Saeed,*[b] Gamal M. El-Mahdy [c] and Hamad A. Al-Lohedan[a]

[a] *Surfactants research chair, Chemistry department, college of science, King Saud University, Riyadh 11451, Saudi Arabia. Fax: 00966114675998; Tel: 00966561557975; E-mail:(A.M. Atta aatta@ksu.edu.sa; H.A. Al-Lohedan hlohedan@ksu.edu.sa).*
[b] *Petroleum Application Department, Egyptian Petroleum Research Institute, Nasr City 11727, Cairo, Egypt. Fax: 0020222747433; Tel: 0020222747917; E-mail: (A.E. El-saeed ashrfelsaied@yahoo.com).*
[c] *Chemistry Department, Faculty of Science, Helwan University, Helwan, Egypt.*

Abstract: The present work aims to develop a method for preparation of porous iron oxide nanomaterials and to investigate the applicability as smart self-healing protective coatings for steel. In this respect, iron oxide nanoparticles doped with iodine and capped with natural modified rosin surfactant were prepared and applied as self- healing materials to repair the cracks of epoxy coats. The mechanism of self- healing characteristics of porous nanomaterials was elucidated using different analyses. The results suggested the formation of stable thin films on the cracks and holes of epoxy coats. Polarization and electrochemical impedance spectroscopy showed an improvement in the corrosion resistance of the epoxy coating. The presence of nanoparticles was found to be an effective in restricting the penetration of aggressive ions by forming a strong barrier layer at coating metal interface.

1. Introduction

Coating of steel is one of the most useful and preferred methods used to protect steel from marine corrosion and fouling [**1**]. In the past, the toxic paints were the main choice for marine coatings due to their ability to kill organisms that settle on the steel coating surfaces. These paints contained lead, copper, arsenic, mercury and their organic derivatives, which have been prevented due to environmental risks [**2-5**]. The antimicrobial nanomaterials hybrid organic coatings based on silicon, carbon black, silver, iron oxides, zinic oxide and titanium dioxide are being used as a best choice to replace the conventional organic coatings [**6-12**]. Moreover, epoxy coatings are most widely organic coating that used to protect steel from corrosion due to their high barrier properties **[13]**. The main disadvantage of the cured epoxy resin is the creation of holes and defects over the coating surface due to high crosslink density of the epoxy networks [**14-16**]. However, the coating deterioration was caused from increasing the depth of these holes and defects after exposure to the corrosive electrolyte [**14–16**]. Currently, nanomaterials are extensively used to modify the barrier effect and the coating performance due to their unique mechanical, biological, magnetic, electrical and optical and properties. Consequently, nontoxic nanomaterials as pigments are being are the best choice to improve the epoxy coating resistance due to their small size, high surface area and their high barrier properties [**17**]. Nano-particles can fill up the holes, micro cracks and defects of organic coatings to boost interactive forces at the polymer filler interfaces **[18]**.

Recently, inorganic well-dispersed nanoparticles particulate fillers in epoxy matrix composites have been extensively investigated to modify the application of epoxy in marine organic coatings [**13**]. Magnetite and ferrite materials have been widely used as magnetic layers on polyethylene terephthalate (PET) film, paper or metallic substrate **[19]**. It is expected that the dark colour of nano Fe_3O_4 increases its application as an excellent inorganic pigment. Moreover, the adhesion and protection ability to polymeric coatings can be enhanced [**20**]. Furthermore, it has also been reported that the magnetite nanocomposites have superior anticorrosive properties [**21-26**]. It was reported that, the selection of the suitable capping agents that based on natural product, particle size distribution and highly dispersed for production of iron oxide are the main factors responsible for their superior anticorrosive materials for steel against aggressive environments. It was found that nanoferrite dispersed waterborne epoxy-acrylate, and magnetic ferrite revealed that the Fe_3O_4 nanocomposite coatings bear a promising potential for commercialization as anti-corrosion protective coating materials [**27, 28**]. It was also demonstrated that, the encapsulation of Fe_3O_4 into the organic coating matrix increases the protection performances of these coatings [**29].**

Furthermore, self-healing composites such as magnetite in polystyrene incorporated microencapsulated healing agents showed excellent levels of healing efficiency in both static and dynamic loading conditions [**30**]. Moreover, magnetic nanoparticles was used as nano-heaters in a self-healing ionomer matrix and succeeded to accelerate effective recovery of the mechanical properties within short time after coating damages [**31**].In the present work, the doping of iodine on the surface magnetite nanoparticles capped with cationic rosin surfactants could enhance their performance to produce stable iron oxide nanoparticles cannot leached from organic coatings and can serve as self- healing materials for damaged coatings. The prepared magnetite nanoparticles were selected to blend with commercial epoxy resin as nano-filler materials to modify the epoxy coating performance against aggressive condition of marine environments. Although the marine environments are highly aggressive for epoxy organic coatings but it was expected that the self- healing characteristics of nanoparticles could be enhance the passivation of steel against corrosive conditions. Rosin was selected as alicyclic natural products to modify the magnetite nanoparticle surface due to its high anticorrosive characteristics as organic coatings as described in our previous works [**32-34].** The measurements of mechanical properties as well as protective efficiency of the magnetite/epoxy nanocomposite as organic coatings for steel against marine environment were investigated using different techniques.

2. Experimental

2.1. Materials

Gum rosin was obtained from Wuzhou Chemical, China and used to prepare bis-*N*-(3-levopimaric maleic acid adduct-2-hydroxy) propyl-triethyl ammonium chloride (LPMQA) as reported in our previous work [**24**]. The commercial epoxy resin SigmaGuard ^{TM} CSF 650 produced by Sigma Coatings, SigmaKalon Group is two component solvent free amine. The mixing ratio between epoxy resin and hardener by volume is 4:1. Anhydrous ferric chloride ($FeCl_3$), potassium iodide, and ammonium hydroxide (28 mass %) were used to prepare iron oxide nanoparticles. Steel specimens having chemical composition (wt.%): 0.14% C, 0.57% Mn, 0.21% P, 0.15% S, 0.37% Si, 0.06% V, 0.03% Ni, 0.03% Cr and the remaining iron were used as panels to apply the epoxy resins as organic coatings. The panels (15 cm x 10 cm) were blasted using emery paper grade 220, 400, 600, 800, and 1200 and 2000. The panels were washed with bi-distilled water, degreased ultrasonically in ethanol, and finally dried at room temperature before application of epoxy and epoxy iron oxide nanocomposites as organic coatings.

2.2. Preparation of capped irom oxied nanoparticles

The iron oxide capped with LPMQA was prepared by mixing of 13.2 g (0.08 mol) potassium iodide dissolved in 50 ml of distilled water with 40 g of anhydrous $FeCl_3$ solution in 300 ml under stirring at room temperature. The solution was heated slowly up to 50 ^{o}C and LPMQA (5 g in 100 ml of water) was added dropwise at the same time with 200 mL of ammonia solution (28 %) to the reaction mixture. The reaction was completed at temperature of 50 ^{o}C under stirring for 4 h. The iron oxide nanoparticles doped with iodine and capped with LPMQA were purified after isolation by ultracentrifuge at 15,000 rpm for 30 minutes by washing five times with ethanol. The product was designated as Fe_3O_4 / LPMQA / I_2.

2.3. Preparation of epoxy/magnetite nanocomposite coats

Different weight ratios of Fe_3O_4 / LPMQA / I_2 (0.1, 1 and 10 Wt % related to the total weight of epoxy and hardener) were mixed with epoxy resins using ultra-sonication rod with power of 25 % for 25 min. The polyamine hardener was mixed with dispersed epoxy/magnetite solution at mixing ratio 4:1 of epoxy: hardener. The mixture was applied on the blasted and cleaned steel panels (15 cm x 10 cm) by means of a conventional spraying to obtain dry film thickness (DFT) of 100 ± 10 µm after curing at room temperature for 6 hrs. The blank cured epoxy coat was obtained by mixing epoxy to hardener without adding Fe_3O_4 / LPMQA / I_2 using the above mentioned procedure.

2.4. Characterization of Epoxy/iron oxide nanocomposites

2.4.1 Capped iron oxide nanoparticles

Fourier transform infrared (FTIR; model Nicolet FTIR spectrophotometer) was used to elucidate the doping and capping of Fe_3O_4 / LPMQA / I_2.

The morphologies of the prepared Fe_3O_4 / LPMQA / I_2 nanoparticles were investigated using transmission electron microscopy (TEM; model JEOL JEM-2100F; JEOL, Tokyo, Japan) at acceleration voltage of 200 kV.

High resolution scanning electron microscopy (SEM, model JSM-T 220A, JEOL) used to study the surface morphologies of epoxy nanocomposite coats using an accelerated voltage of 20 kv.

Type of crystalline iron oxide nanoparticles was determined from X-ray powder diffraction (XRD) patterns were recorded using a D/max 2550 V X-ray diffractometer (XPert, Philips, Eindhoven, The Netherlands) with Cu Kα radiation of wavelength 1.54 Å, operating at a voltage of 40 kV and a current of 40 mA at a rate of 2◦ min^{-1} and in the range 2θ = 0–80◦.

Thermal stability of the prepared Fe_3O_4 / LPMQA / I_2 determined from thermogravimetric analysis (TGA; Universal V3.5B TA instruments) from room temperature to 850 °C under heating rate of 10 degree/ min in nitrogen atmosphere.

2.4.2. Antimicrobial activity of iron oxide nanoparticles

Antimicrobial effects, minimum inhibitory concentration (MIC) and minimum bactericidal concentration (MBC) of the iron oxide nanoparticles were determined using the broth-micro dilution test against three common strains of bacteria; Escherichia coli ATCC 8739, Staphylococcus aureus ATCC 6538, Bacillus subtilis ATCC 6633 and Pseudomonas aeruginosa ATCC 10145. More details about the evaluation of antimicrobial test on the magnetite were reported in previous work [**35**].

2.4.3. Mechanical resistance of coated epoxy nanocomposites films

The mechanical properties of cured epoxy nanocomposite films in the presence or absence of Fe_3O_4 / LPMQA / I_2 nanoparticles on the steel panels were carried out according to appropriate ASTM standard test methods as reported in previous work **[36].** The steel panels were blasted and cleaned according ASTM D 609-00. The adhesion pull-off test determined using a hydraulic pull-off adhesion tester in the range of 0–25 MPa. The hardness was determined by using Erichsen hardness test pencil, model 318S, scratching force in the range of 0.5–20 N. The abrasion resistance was evaluated according ASTM D4060-07 by applying 5000 cycles with 1000 g load on the tested panels. A salt spray cabinet (manufactured by CW Specialist equipment ltd. model SF/450) was used to evaluate the salt spray resistance of coated panels.

2.5. Corrosion resistance of epoxy films

Corrosion protection properties of the epoxy coating samples were investigated by OCP, potentiodynamic polarization and EIS analysis. Electrochemical measurements were conducted using Solartron 1470E (multichannel system) as electrochemical interface and the Solartron 1455A as FRA. Polarization measurements were conducted at different time immersions in 3.5% NaCl solution using a scan rate of 1mV/Sec. Three electrodes cell configuration was used to study the electrochemical corrosion behaviour of coated materials. Ag/AgCl was used as reference electrode, platinum as auxiliary and test specimen as working electrode. The exposed area of the working electrode was 1.0 cm^2. EIS measurements were made at open circuit potential with 10 mV amplitude of the sinusoidal voltage signal at applied frequencies in the range of 10 KHz–10m Hz using 10 points per decade.

3. Results and Discussion

It was previously reported that that magnetite, other iron oxides, mixed oxides of iron and copper have strong ability to form passivating anticorrosive film on steel in the expected repository environment [**37, 38**]. The stability and solubility of these passivating films affect their protective performances on the steel surfaces. However, the solubility of magnetite in water depends on different parameters, such as temperature, pH and the presence of complexing agents. Moreover, the transformation of magnetite to other iron oxide reduces its ability for passivation the steel surfaces. In this work, the stable magnetite nanoparticles capped with cationic surfactant based on rosin can be used to prepare highly dispersed epoxy nanocomposite as anticorrosive coatings for steel. Moreover, the possibility of magnetite epoxy nanocomposite to form other types of passivating films as well as its mechanism for self-healing of coating defects on the steel surface will be discuss in the forthcoming section. Moreover, the mechanical properties and

protective characteristics of epoxy nanocomposites have therefore been studied.

3.1. Characterization of magnetite / LPMQA nanoparticles

In previous work magnetite nanoparticles capped with LPMQA were prepared by reacting of $FeCl_3$ with KI to produce iron cations and iodine **[24]**. The magnetite nanoparticles were prepared after hydrolyzing the iron cations with ammonia solution after removal of iodine precipitate. In the present work, the magnetite nanoparticles capped with LPMQA can be also prepared by hydrolysing of iron cations without removal of iodine from the reaction medium as reported in the experimental section. The presence of iodine in the reaction medium is very important to control the particle size of different iron oxide nanoparticles [**25, 26].**

The chemical structure of iron oxide nanoparticles capped with LPMQA surfactants in the presence of iodine was confirmed from FTIR analysis as represented in **Fig. 1.**

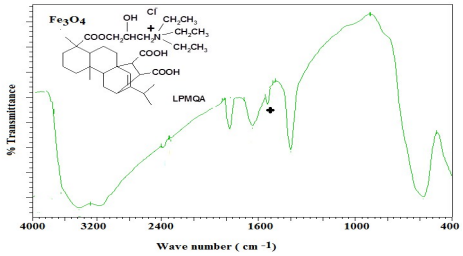

Fig. 1. FTIR spectrum of magnetite capped with LPMQA surfactant in the presence of iodine.

The formation of iron oxides was elucidated from the absorption bands in the region of 400-800 cm $^{-1}$. The appearance of broad band at 570 cm^{-1} that referred to Fe–O stretching vibration confirms that only Fe_3O_4 as iron oxides was produced. Moreover, the band at 3455 cm^{-1} refereed to the stretching vibrations of –OH, elucidates the modification of Fe_3O_4 surfaces with OH groups. The bands appeared at 2885 and 2925 cm^{-1} that attributed to C–H stretching vibration, 1720 cm^{-1} attributed to C=O stretching of ester, band around 1371 cm^{-1} assigned to C–N stretching vibration confirm the capping of magnetite with LPMQA surfactant. The new band at 1537cm^{-1}, which was not appeared in previous work [**24**] for capping of magnetite with LPMQA in absence of iodine, elucidates that the iodine was doped on the magnetite surface layers [**39].**

FTIR analysis indicates that magnetite was capped with LPMQA surfactant and doped with iodine. The removal of the uncapped LPMQA surfactant on the magnetite was confirmed from measuring the surface tension of the washed magnetite nanoparticle filtrate to be 73 m/Nm at 25 ^{o}C. The content of LPMQA surfactant capped on the magnetite can be determined from TGA data listed in **Table 1**.

Table 1. TGA data of magnetite capped with LPMQA surfactant in the presence of iodine.

Steps		Weight Loss (%)	IDT (^{o}C)	T_{10}% (^{o}C)	Y (%)		
Start Temp. (^{o}C)	End Temp. (^{o}C)				650 (^{o}C)	750 (^{o}C)	850 (^{o}C)
0	250	5.5	35	340	83	80.5	73
250	450	9					
450	650	2.5					

The initial decomposition temperature (IDT) at 35 ^{o}C confirms the presence of non-bonded water. Moreover, the weight loss percentage (5.5 Wt %) at the temperature range 25 to 250 ^{o}C confirms the dissociation of water and iodine from the magnetite surface capped with LPMQA surfactant. The weight loss percentage (9 wt %) at temperature range of 250 to 450 ^{o}C referred to decomposition of LPMQA surfactant confirms the LPMQA content that capped on the magnetite surface. The residual percentage (Y %) remained at 650, 750 and 850 ^{o}C was used to determine the magnetite content and dissociation of magnetite to other iron oxides [**40**]. The data indicate the magnetite content equals 83 wt. %.

The iron oxide type and its crystal structure can be elucidated from XRD diffractograms as illustrated in **Fig. 2**. The appearance of peaks at 2θ equal to 20.1, 29.9^{o}, 33.13^{o}, 43.2^{o}, 53.5^{o}, 57.1^{o}, and 62.7^{o} can be indexed as (111), (220), (311), (400), (422), (511) and (440), respectively indicates that pure magnetite was formed without contamination of other iron oxides [ref. code 00-003-0863]. Moreover, the presence of these diffractions elucidates that the Fe_3O_4 crystal has a cubic spinel structure. The crystal size of Fe_3O_4 nanocrystallites can be calculated using Scherrer's formula:

$$d = 0.94\lambda/\beta \cos\theta \qquad (1)$$

Where d , θ, β are the crystallite size, position of the Bragg peak and the half-width of the strong diffraction peak at 2-theta 33.13^{o} that represents (311).

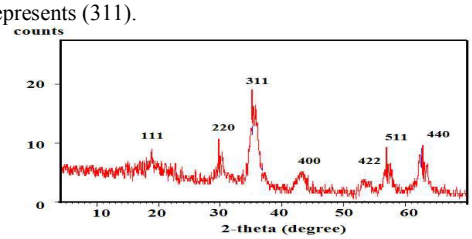

Fig.2. XRD diffractogram of magnetite nanoparticles capped with LPMQA surfactant in the presence of iodine.

The measured mean size of the magnetite capped with LPMQA surfactant in the presence of iodine equals to 18.1 ± 0.7 nm.

High resolution transmittance electron microscope (HR-TEM) can be used to illustrate the morphology of magnetite capped with LPMQA surfactant in the presence of iodine as represented in **Fig. 3**. An interesting observation was noticed for capped magnetite nanoparticles morphology (Fig**. 3**) that shows dispersed spherical porous nanoparticles of 10-20 nm in size. The pore size was roughly estimated from HR-TEM to be ca. 0.5 nm from TEM image (Fig. 3). It is well known that the pore sizes were rough estimated by TEM at irregular pores. However, the porosity of magnetite nanoparticles capped with LPMQA surfactant in the presence of iodine refers that iodine assists the self-assemble of LPMQA on the magnetite surfaces [**40**]. Such self-assemble on the surface of non-spherical particles has excellent building blocks for effective creation of surfaces of high roughness [**40**]. This behaviour can also benefit the lustiness of organic coatings by interlacing with each other to protect the coating surfaces from damage and corrosive environments.

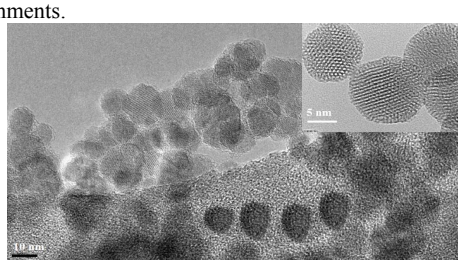

Fig.3. HR-TEM micrograph of magnetite nanoparticles capped with LPMQA surfactant in the presence of iodine.

The antimicrobial activity of magnetite nanoparticles capped with LPMQA surfactant in the presence of iodine against grams positive and negative bacteria is very important to measure as listed in **Table 2**.

Table 2. Minimum inhibition concentration (MIC) and the % reduction of organism for 10, 5, 2.5, and 1 mg mL^{-1} of samples against *Escherichia coli* ATCC 8739, *Staphylococcus aureus* ATCC 6538, *Bacillus subtilis* ATCC 6633, *Pseudomonas aeruginosa* ATCC 10145 strains.

Antimicrobial materials	MIC (µg mL^{-1})	The reduction of organism (%)				
		0.5 µg mL^{-1}	1 µg mL^{-1}	2.5 µg mL^{-1}	5 µg mL^{-1}	10 µg mL^{-1}
E. coli	10		44±6	61±2	77±5	93±7
S. aureus	5	-	-	39±4	92±4	98±2
B. subtilis	2.5	31±8	64±7	95±3	96±2	98±2
P. aeruginosa	5	29±4	64±5	86±4	92±4	95±5

In this respect, the minimum inhibitory concentration (MIC; µg mL^{-1}) using different types of gram positive (Staphylococcus aureus ATCC 6538 and Bacillus subtilis ATCC 6633) and negative (Escherichia coli ATCC 8739 and Pseudomonas aeruginosa ATCC 10145) bacterial strains are used to evaluate the antimicrobial activity of magnetite nanoparticles. These types of bacteria were widely used to bacterial experiment because they are living on the body surface of mammals or in water and they are harmful and sometimes cause infection to them [**41].** The data (Table 2) confirm the high antimicrobial activity of the prepared nanoparticles against both types of bacteria strains. These data confirm the presence of both doped iodine and capped LPMQA surfactant on the surface of magnetite nanoparticles that enhance the attack of nanoparticles on the bacteria walls and prevent their growth. It was previously reported that the antimicrobial activity of magnetite was refereed to their ability to form superoxide and hydroxide radicals on their surfaces and consequent cause damage to proteins, membranes and DNA of bacteria strains [**42, 43**]. Moreover, the smaller size of magnetite nanoparticles than bacterial pores increases their ability of crossing the cell membrane, disrupting its function or interfering with nucleic acid or protein synthesis [**44**]. The effective MIC values ranged from 2.5 to 10 µg mL^{-1} indicate that the prepared nanoparticles have the most intensive the antimicrobial activity than reported for other magnetite nanoparticles [**42-44**].

3.2. Mechanical properties of magnetite hydride epoxy nanocomposite coats

It is well reported that the curing of the epoxy resins with polyamines produces high crosslinked networks contains ether and hydroxyl groups [**45**]. The presence of nanoparticles improves the crosslink density via formation either physical or chemical bonds with the networks [**46].** In the present work the scheme of crosslinking of epoxy resin and polyamines in the presence of magnetite nanoparticles capped with LPMQA surfactant was represented in **Scheme 1**. The presence of LPMQA surfactant on the surface of magnetite facilitates the physical and chemical interactions with either epoxy resin or polyamine hardener. The crosslinking of epoxy was confirmed by testing the resistance of films to methyl ethyl ketone(MEK). All films were not solubilize or affected MEK. The expected interactions can be confirmed from SEM micrographs as represented in **Fig. 4**. The formation of highly crosslinked networks of the cured epoxy resin and polyamine confirmed in **Fig. 4a** that elucidates the formation of a minor micro cracks on the surface of the solid cured epoxy coating in the absence of magnetite nanoparticles. **Fig. 4b** shows that the

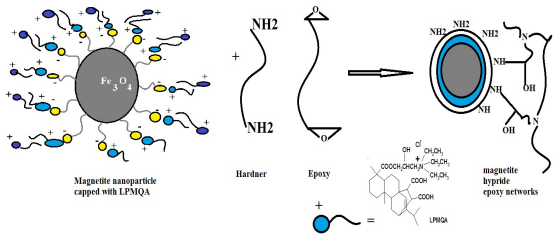

Scheme 1. Curing of magnetite capped with LPMQA surfactant in the presence of iodine with epoxy resin and polyamine hardener.

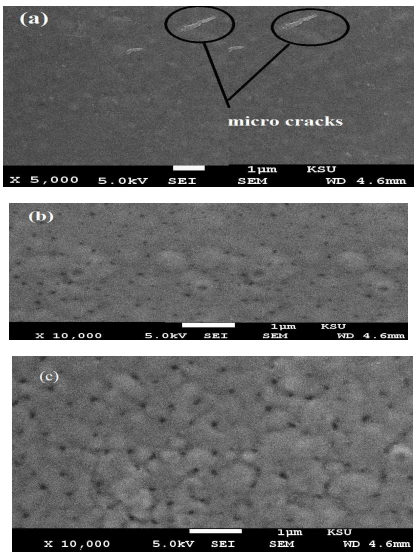

Fig.4. SEM micrographs of epoxy nanocomposite a) blank, b) blended with 0.1Wt % and c) blended with 1 Wt. % of magnetite nanoparticles.

magnetite coated with LPMQA surfactant improves the crosslink density of the epoxy networks via formation of well dispersed magnetite nanoparticles with cured networks. Moreover, no agglomeration was detected for modified epoxy magnetite nanocomposites as shown in **Fig. 1(b)**. This can be referred to the presence of LPMQA surfactant on the magnetite surface, which decreases Van der Waals forces between magnetite nanoparticles and increases the repulsion between magnetite nanoparticles. The capping of LPMQA surfactant on the magnetite surface prevents their agglomeration by adsorbing on the suspended particles surfaces, providing steric hindrance and an electrostatic barrier to agglomeration [**47**]. Moreover, the presence of carboxylic and hydroxyl groups on the surface of the magnetite particles (**scheme 1**) provides locations for the polar basic groups of the dispersant to interact with epoxy and polyamine. **Fig. 4c** confirms that the increment of magnetite weight percentage from 0.1 to 1 Wt. % added some minor agglomerates with increasing of the magnetite nanoparticles in the epoxy networks. The minor agglomeration is created by both van der Waals forces and electrostatic attraction of the charges present on the surface of the particles. SEM micrographs (**Fig. 4 b and c**) showed a fine uniform dispersion of magnetite nanoparticles with smooth and flat overlapping structure without formation of micro or nano cracks.

It is therefore of cardinal importance to investigate the mechanical properties of the cured epoxy polyamine system in the presence and absence of the different weight contents of magnetite nanoparticles. The hardness, T-bending, impact and

abrasion resistance of these coats were determined as described in the experimental section and represented in **Table 3**. It is very important to evaluate the mechanical properties of these coats

Table 3. Mechanical properties of epoxy/magnetite nanocomposites.

Nanoparticles %		Hardness (N)	Adhesion (MPa)	Impact (Joule)	Abrasion Resistance weight loss (mg)
blank		3	3	5	65
Fe_3O_4/ LPMQA/I_2	0.1	5	9	9	25
	1.0	6	12	12	18
	10	9	16	16	11

(such as harness, impact and abrasion resistances) with their adhesion on the steel surface. The adhesion of coats with steel was determined by measuring the pull-off forces and represented in Table3. The data indicate the increment of the magnetite nanoparticle contents increases the adhesion of the epoxy networks with steel. This may be attributed to the presence of more reactive functional groups such as hydroxyl, produced from the system Fe-O-H, epoxy and LPMQA surfactant, ether and carboxylic groups will increase their complexing as organic ligand with steel surfaces. The data listed in Table 3 of superior adhesion of epoxy with steel in the presence of capped magnetite nanoparticles confirms the good dispersability of iron oxide nanoparticles in the films. This in turn provides higher cross-linking density, improved thermal and chemical resistance properties of epoxies [**48**]. The data listed in **Table 3** elucidate the increment of impact resistance of cured epoxy resins with increasing the iron oxide contents. This referred to the greater interaction between magnetite nanoparticles and epoxy polymer matrix will reduce the impact stresses, which transferred from the polymer matrix into the iron oxide nanoparticles. This was confirmed from the absence of micro or nano-cracks for cured epoxy coats as confirmed from SEM micrographs (Fig**. 4**). The increment of film hardness with increasing the magnetite nanoparticles contents confirms the increasing of the crosslink density of epoxy network with increasing the magnetite contents. This indicates that the epoxy coating reinforced with the nano sized particles by the chemical and physical interactions among particles and the coating matrix that increases the abrasion resistances of coats as illustrated in **Table 3**.

3.3. Salt spray resistance of epoxy/magnetite nanocomposite coatings

The adhesion pull of resistance of the epoxy magnetite nanocomposite coats indicates that the adhesion of epoxy that increased more than 5 MPa. The mechanical properties data indicated that the present system can be applied as protective coatings for steel from corrosive marine environment [**49, 50**]. In this respect, the salt spray resistance of the epoxy coatings were evaluated after exposure to 1000 h and listed in **Table 4**.

Table 4. Salt spray resistance of epoxy magnetite nanocomposites.

Nanoparticles %		Disbonded area		Rating Number (ASTM D1654)
		cm^2	%	
Blank		16.5	9	6
Fe_3O_4/ LPMQA/I_2	0.1	1.6	1	9
	1.0	0.1	0.01	10
	10	0.2	0.1	10

The experiment of salt spray resistance was conducted in aggressive marine condition using 5 Wt. % sodium chloride solutions at pH range of 6–7. The coated specimens were subjected to diagonal scratch using sharp knife in order to expose the base metal to continuous salt fog at high humidity up to 1000 h. Salt spray test give the macro morphology of coats even no visual blisters. Visual inspection of the tested specimens did not show any visual blisters or rusts near scribes and at the coating/metal interface except the blank sample that coated without addition of magnetite nanoparticles. This indicates that magnetite nanoparticles could enhance the epoxy coating anti-corrosion performance significantly.

SEM micrograph used to verify the corrosion products formed on the surface of the scratched coated steel sample with epoxy / magnetite nanocomposite as represented in **Fig. 5**. The SEM micrograph indicates that there is a uniform porous protective film formed on the surface of the steel. This means that the magnetite nanomaterials doped with iodine and capped with LPMQA have strong ability to repair the scratch epoxy coating in the marine corrosive environment. This may prove that the magnetite nanomaterials can act as a pigment to protect the steel surface through forming protective layer.

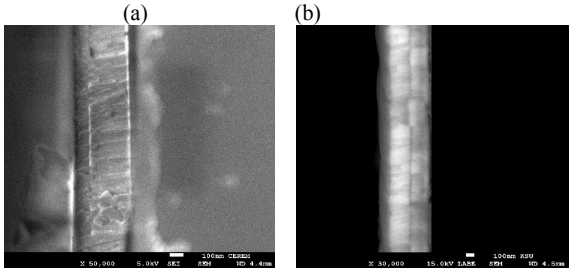

Fig.5 . SEM of damaged epoxy/magnetite nanocomposites with a) 1 Wt % and b) 10 Wt % of

The mechanism for formation of protective film can be described in the following equations:

$$2H_2O + O_2 + 4e^- \longrightarrow 4OH^- \text{ (pH} \uparrow\text{)} \quad (2)$$

$$Fe_3O_4 + 2OH^- \longrightarrow 3FeOOH + 2H^+ \text{ (pH} \downarrow\text{)} \quad (3)$$

$$3Fe(s) + 4I_2(aq) \longrightarrow Fe_3I_8(aq) \quad (4)$$

$$Fe_3I_8(aq) + 4Na_2CO_3(aq) \longrightarrow Fe_3O_4(s) + 8NaI(aq) + 4CO_2(g) \quad (5)$$

$$2Fe_3O_4 + OH^- \longrightarrow 3\gamma\text{-}Fe_2O_3(s) + H^+ \quad (6)$$

The presence of salt increase the pH of solution based on electrochemical reaction that occurs beneath the coating resulting in hydroxyl ions (OH−) creation as illustrated in equations 2 and 5. The hydroxyl ions and sodium carbon exists in sea water can diffuse into the epoxy network to catalyze the hydrolytic degradation and etheric bonds cleavage of epoxy networks [**51, 52**]. The presence of magnetite nanoparticles at low crosslinking density of epoxy network areas leads to a decrease in the electrolyte diffusion into the coating matrix through equation 3 to produce goethite and decrease in pH in the coating matrix [**51**]. Moreover, the presence of iodine on the surface of magnetite nanoparticles can react with the scratched steel and forming intermediate according to reaction of equation 4. The formed intermediate can react with the (OH−) or Na_2CO_3 to form magnetite and maghemite which are more stable to leach from coatings that will protect the scratch area (equations 5 and 6) [**53**]. The self-healing capacity of the coating appeared to be due to the release of iodine capped on the magnetite particle surfaces as a result of the increase in pH that resulted from both the cathodic reaction during corrosion and the formation of a film on the defect (scheme 2).

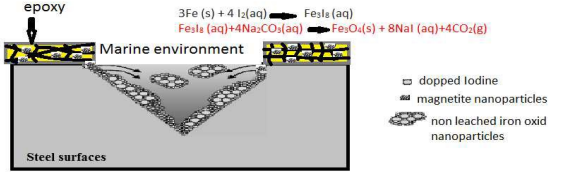

Scheme 2: Mechanism of self-healing of Fe_3O_4/ LPMQA/I_2 nanoparticles in sea weater conditions.

3.4. Electrochemical tests

3.4.1. Open circuit potential (OCP) measurements

OCP measurement is a simple additional tool, which provides information about the coating corrosion resistance and the corrosion resistance of underlying substrate after exposure to aggressive solutions [**54**]. Monitoring data of the OCP values of the scratched epoxy coating without and with additions of Fe_3O_4 / LPMQA / I_2 nanoparticles are illustrated in **Fig.6**. During the exposure time, the OCP values of epoxy coating without additions of nanoparticles continuously decreases toward more negative potential, which give rise to an active corrosion process. In case of coating containing different concentrations of nanoparticles, the OCP shifts to less noble values during the initial time of immersion and slowly tends to noble values and eventually attains a steady state during the last stage of immersion. It can be seen that less steep decline to negative direction of OCP experienced during monitoring the OCP data in presence of 0.1 Wt % than that displayed at higher one (1 Wt %). The results can be attributed to formation of more corrosion products in presence of 1 Wt %, which fill the scratched area and causes a shift in OCP values to more noble values. The OCP behaviour remained constant after 200 hours exposure due to the entire filling of the scratched area with corrosion products as well as saturation limit of the film. The drop in OCP levels the blank samples indicates that water and ions penetrate the coating, and causes corrosion of underlying substrate. The gradual decrease in OCP for blank sample may be attributed to the diffusion of water and the Cl^- ions at the coating/steel interface, which in turn increases the corrosion reaction of underlying substrate and causes a sharp drop in OCP.

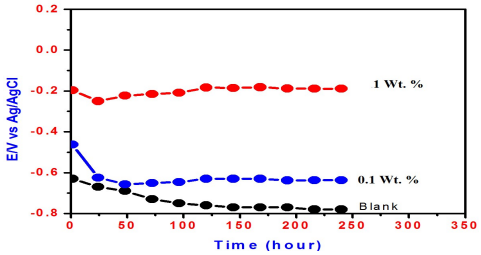

Fig. 6. Influence of nanoparticle content on the OCP monitoring data for epoxy/magnetite nanocomposites.

3.4.2. Polarization measurements

Polarization curves of the scratched epoxy coating without and with additions of Fe_3O_4 / LPMQA / I_2 nanoparticles are shown in **Fig. 7**. Electrochemical parameters obtained from the plots like Ecorr, Icorr, anodic (ba) and cathodic Tafel slopes (bc) are provided in **Table 5**. It is clear that, Ecorr was shifted towards the noble direction for the coated samples contain Fe_3O_4 / LPMQA / I_2 nanoparticles. In addition, I_{corr} values for coated samples containing Fe_3O_4 / LPMQA / I_2 were found to be lower than that of Blank sample and decreased with increasing the concentration of nanoparticles. The results indicated that the additions of Fe_3O_4 / LPMQA / I_2 nanoparticles provide protection to the coated sample against corrosion in the chloride containing environments. In addition, as the immersion time increased a considerable decrease in corrosion rate was observed. The result can be accounted to the presence of Fe_3O_4 / LPMQA / I_2 nanoparticles, which facilitates the precipitation of the corrosion products on of the scratched coating (self-healing) and enhances the adhesion between coating and steel surface resulting in an enhancement the corrosion resistance performance of these coatings. Moreover, Fe_3O_4 / LPMQA / I_2 nanoparticles stimulates a barrier and screen effect at coating-steel interface that shifted the corrosion potential in more noble direction followed by the reduction in their corrosion current density [**55**], thus stimulate the corrosion protective efficiency of these coatings [**56**]. It can be concluded that the presence of higher amount of Fe_3O_4 / LPMQA / I_2 nanoparticles within the coating material provides a strong barrier at coating-steel interface by filling the scratched area on the coating surface with large amounts of corrosion products, which did not allow the penetration of corrosive ions (Cl^-) to the coating steel interface. As a consequence, it enhances the corrosion protection performance of coatings in presence of higher amount of Fe_3O_4 / LPMQA / I_2 nanoparticles.

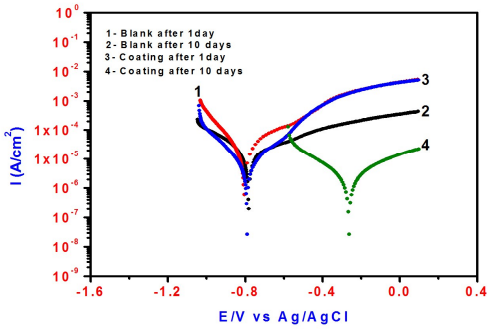

Fig. 7. Influence of nanoparticle content on the polarization curves for the epoxy coating measured at different immersion times in 3.5% NaCl solution.

Table 5: Electrochemical parameters for the epoxy coating blended with (0.1 Wt. % of magnetite nanoparticles) calculated by polarization and EIS methods at different immersion time.

Samples	Polarization Method				EIS Method
	ba (mV)	bc (mV)	E_{corr} (V)	i_{corr}, $\mu A/cm^2$	$R_p \times 10^5$ Ohm
Blank after 1 day	193	356	-0.7829	38.6	0.06186
Blank after 10 days	191	146	-0.8054	17.7	0.09021
Fe_3O_4 / LPMQA / I_2 (1 day)	211	178	-0.7913	7.01	0.2683
Fe_3O_4 / LPMQA / I_2 (15 days)	428	357	-0.2632	3.91	0.53344

3.4.3. Evaluation of impedance spectra during exposure time

EIS has been employed to monitor and predict the degradation of paint coatings [**57-59**]. The impedance spectra of the epoxy coating immersed in 3.5% NaCl solution without and with Fe_3O_4 / LPMQA / I_2 are shown in **Fig. 8**. The difference in impedances measured at low and high frequencies was used to determine polarization resistance [**60**]. It can be concluded that the specimen containing high percent 1 Wt. % of nanoparticles coated has a higher impedance values than the other samples since the diffusion process is limited due to barrier effect of Fe_3O_4 / LPMQA / I_2 nanoparticles. The addition of nanoparticles accelerated the self-healing and limited the penetration of corrosive ions into coating/steel interface. Many blisters were observed around the scratched area in blank sample indicating the ingress of water and the aggressive ions into the steel/coating interface. As a consequence, the adhesion of coating decreased and facilitates the penetration of ions and accompanied by a degradation of the coating.

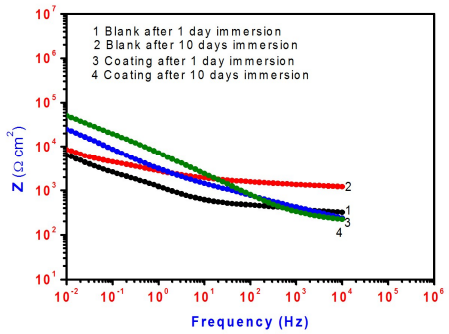

Fig. 8. The Bode plots of epoxy coating with different percent of nanoparticles at different immersion times in 3.5% NaCl solution.

These results obviously show that the sample incorporating with nanoparticles has better protection performance towards corrosion in chloride containing environment than that experienced by the blank sample. As the corrosive electrolyte penetrates to the underlying substrate, the electrochemical reactions initiates at active sites of the scratched surface. The created hydroxyl ions (OH^-) at cathodic regions ($2H_2O + O_2 + 4e^- = 4OH^-$) increases and the pH beneath the coating increases and causes a destruction of the coating from the substrate. The samples containing nanoparticles showed better barrier performance as the immersion time elapsed. The results presented in **Fig. 8** showed that the impedance values increased significantly in the presence of nanoparticles, which in turn increased the coating resistance in the chloride containing environment. Healing of scratched area provides partial or complete surface coverage with corrosion products, which act as an effective barrier to prevent corrosion. Coating sample with low percent of Fe_3O_4 / LPMQA / I_2 produced little amount of corrosion products, which repair the scratched active sites and did not completely prevent the corrosion process. In case of coating samples with high percent of Fe_3O_4 / LPMQA / I_2 nanoparticles the amount of the corrosion products increased to be enough to seal the scratched active sites. The improvement in the scratched corrosion resistance properties loaded with nanoparticles can be attributed to the spinel structure of Fe_3O_4 nanoparticles. The increase in the self-healing ability of the loaded coating with nanoparticles can be attributed to the presence of oxygen at corners of the cubes and iron at octahedral and tetrahedral positions, which induces higher adhesion with the scratched coating, leading to an improvement in the scratched coating corrosion resistance performance. The addition of Fe_3O_4 nanoparticles in the coating film provides a strong barrier layer, which inhibits the penetration of electrolyte and improves the corrosion protective performance of the loaded coatings film with nanoparticles. It can be concluded that the additions of nanoparticles greatly lower the corrosion process of the underlying substrate by providing a long path for aggressive ions diffusion and successfully protect the underlying substrate.

4. Conclusions and outlook

Pure porous antimicrobial magnetite nanoparticles having narrow particle size of 15 nm were prepared using LPMQA surfactant as capping agent. The LPMQA was capped magnetite with 11.5 Wt. % and iodine was doped on the surface of the magnetite. The mechanical properties of the epoxy were improved by adding small content (0.1 Wt. %) of the magnetite nanomaterial. The corrosion resistance of the coating was increased in the presence of 1 Wt. % of nano sized Fe_3O_4 / LPMQA / I_2. The highest adhesion was also recorded at the same content. It was found that, the presence of doped iodine on the surface of magnetite is responsible for coating resistance against hydrolytic degradation of epoxy coatings in marine environment. The presence of higher amount of Fe_3O_4 / LPMQA / I_2 nanoparticles within the coating material provides a strong barrier at coating-steel interface and enhances the corrosion protection performance of coatings. The anti- corrosion performance, high salt spray resistances and high antimicrobial activities of the coating reinforced with the nano Fe_3O_4 / LPMQA / I_2 recommended applying as marine coatings of steel.

Acknowledgment

This project was supported by King Saud University, Deanship of Scientific Research, Research Chair.

Notes and references

1. D.M. Yebra, S. Kiil and K. Dam-Johansen, *Progress in Organic Coatings*, 2004, 50, 75-104.
2. E. Almeida, T. C. Diamantino and O. deSousa, *Progress in Organic Coatings*, 2007, 59(1), 2-20.
3. L.D. Chambers, K.R. Stokes, F.C. Walsh, R.J.K. Wood, *Surface and Coatings Technology*, 2006, 201(6), 3642-3652.
4. S. Kiil , C. E. Weinell, D. M. Yebra and K. D.Johansen, *Computer Aided Chemical Engineering*,2007,23,181-238.
5. E. B. Kjaer, *Progress in Organic Coatings*, 1992, 20, 339-352.
6. S. A. Kumar, M. Alagar and V. Mohan, *Surface Coatings International Part B: Coatings Transactions*, 2001, 84, 43-47.
7. O.D. Lewisa, G.W. Critchlow, G.D. Wilcox, A. deZeeuw and J. Sander, *Progress in Organic Coatings* ,2012,73 , 88– 94.
8. D.K. Chattopadhyay, A.D. Zakula and D.C. Webster, Progress *in Organic Coatings* ,2008,64 , 128-137.
9. S. A. Kumar and A. Sasikumar, *Progress in Organic Coatings*, 2010, 68, 189–200.
10. B. Ramezanzadeh and M.M. Attar, *Progress in Organic Coatings*, 2011, 71 , 314–328.
11. X. Zhang, F. Wang and D. Yuanlong, *Surf. Coat. Technol.*,2007,201,7241–7245.
12. S.K. Dhoke and A.S. Khanna, *Corrosion. Science*, 2009, 51, 6–20.
13. C.A. May (Ed.), Epoxy Resins – Chemistry and Technology, 2nd ed., MarcelDekker, NewYork, 1988.
14. V.B. Miskovic-Stankovic, M.R. Stanic and D.M. Drazic, *Progress in Organic Coatings*, 1999, 36 ,53–63.
15. H.L. Yang, F.C. Lin, E.H. Han, *Progress in Organic Coatings*, 2005, 53, 91–98.
16. S.K. Dhoke and A.S. Khanna, *Mater. Chem. Phys*. 2009, 117, 550 –556.
17. M. Nematollahi, M. Heidarian, M. Peikari, S.M. Kassiriha, N. Arianpouya and M. Esmaeilpour, *Corrosion Science*, 2010, 52, 1809–1817.
18. D. Y. Wu, S. Meure, D. Solomon, *Progress in Polymer Science,* 2008, 33, 479-522.
19. S. Tochihara, *Progress in Organic Coatings*, 1982, 10, 195 - 204.
20. M.A.A. El-Ghaffar, N.M. Ahmed and E.A. Youssef, *J. Coat. Technol. Res*. ,2010,7 703–713.
21. G.A. El-Mahdy, A.M. Atta and H. A. Al-Lohedan, *J. Taiwan Inst. Chem. Eng*., 2014, 45 , 1947–1953.
22. A.M. Atta, O.E. El-Azabawy, H.S. Ismail and M.A. Hegazy, *Corrs Sci* ., 2011,53 , 1680–1689.

23. A. M. Atta , G. A. El-Mahdy, H. A. Al-Lohedan and A. M. El-Saeed, *Molecules*,2015,20, 1244-1261.
24. A. M. Atta , G. A. El-Mahdy , H. A. Al-Lohedan and S. A. Al-Hussain, *Int J. Mol. Sci*.,2014, 15 ,6974-6989.
25. A. M. Atta, , H. A. Al-Lohedan and S. A. Al-Hussain, *Int. J. Mol. Sci*.,2015, 16, 691-693.
26. A. M. Atta, , H. A. Al-Lohedan and S. A. Al-Hussain, *Molecules*, 2014,19, 11263-11278.
27. O. ur Rahman, M. Kashif and S. Ahmad, *Progress in Organic Coatings*, 2015, 80 , 77–86.
28. Y. Liu, S. Wei, H. Tong, H. Tian, M. Liu and B. Xu, *Materials Research Bulletin*,2014, 60, 359–366.
29. P. Montoya, C.R. Martins, H.G. de Melo, I.V. Aoki, F. Jaramillo, J.A. Calderóna, *Electrochimica Acta*, 2014, 124, 100–108.
30. L.P. Ramı´ rez, K. Landfester, *Macromol Chem Phys* 2003, 204(1), 22–31.
31. N. Hohlbein, A. Shaaban, A.M. Schmidt, *Polymer*, 2015, 69, 301–309.
32. A. M. Atta, R.Mansour, M. I. Abdou and A. M. El-Sayed, *Journal of Polymer Research*, 2005, 12, 127-138.
33. A. M. Atta, S. M. El-Saeed and R. K. Farag, *Reactive and Functional Polymers*, 2006,66(12),1596-1608.
34. A. M. Atta, H. M. Bedawy and I.F.Nassar, *Reactive and functional polymers*,2007, 67, 617-626 .
35. R.Betancourt-Galindo, P. Y. Reyes-Rodriguez, B. A. Puente-Urbina, C. A. Avila-Orta, O. S. Rodríguez-Fernández, G. Cadenas-Pliego, R. H. Lira-Saldivar, and L. A. García-Cerda, *Journal of Nanomaterials*, 2014, Article ID 980545, 5 pages.
36 . A. M. Atta , M.I. Abdoua, A. A. Elsayed and M. E. Ragab, *Progress in Organic Coatings* ,2008,63,372–376.
37. H.P. Hermansson, and M. König, A Short Review, SKI Report 01:38, Swedish Nuclear Power Inspectorate, Stockholm 2001.
38. E.M.Field, Second Int. Congr. on Metallic Corrosion, New York, March 11-15 1963.
39. L.M.H. Groenewoud , G.H.M. Engbers, R. White and J.Feijen , *Synthetic Metals*, 2002,125(3),429-440.
40. X. Du, J. He, J. Colloid Interface Sci. 2010, 345, 269-277.
41. R. Danovaro, A. Dell'Anno, , C. Corinaldesi, M. Magagnini, R. Noble, C. Tamburini, M. Weinbauer, Nature, 2008, 454, 1084–1087.
42. A. Azam, A. S. Ahmed, M. Oves, M. S. Khan, S. S. Habib, and A. Memic, *International Journal of Nanomedicine*, 2012, 7, 6003–6009.
43. W. C. Miles, P. P. Huffstetler, J. D. Goff, A. Y. Chen, J. S. Riffle and R. M. Davis, Langmuir ,2011, 27, 5456–5463.
44. T. Gordon, B. Perlstein, O. Houbara, I. Felner, E. Banin, and S. Margel, *Colloids and Surfaces A*,2011, 374, 1–8.
45. E. W. Flick, Epoxy Resins, Curing Agents, Compounds, and Modifiers, NOYES PUBLICATIONS, William Andrew applied science publishers, New Jerssy, U.S.A - 2nd ed (1993) pp.100-250.
46. H. Shi, F. Liu, L. Yang and E. Han, *Progress in Organic Coatings*, 2008, 62 , 359–368.
47. M.F. Smiechowski and V.F. Lvovich, *J.Electroanal. Chem.*, 2005 , 577, 67–78.
48. M. Sangermano, A. Priola, G. Kortaberria, A. Jimeno, I. Garcia, I. Mondragon and G.Rizza, *Macromol. Mater*. Eng., 2007, 292, 956–961.
49. W. J. Yanga, K.Neoh, E. Kang , S. L. Teoc and D. Rittschof, *Progress in Polymer Science*,2014, 39,1017–1042.
50. A.P. Kumar, D. Depan, N. S. Tomer and R. P. Singh, *Progress in Polymer Science*, 2009, 34(6), 479-515.
51. R.A. Larson, E.J. Weber, Reaction Mechanisms in Environmental Organic Chem-istry, CRC Press, Boca Raton, 1994, pp. 105.
52. Y.T. He, S. J. Traina, *Clay Minerals*,2007, 42(1),13-19 ·
53. R. P. Pogorilyi, I. V. Melnyk, Y. L. Zub, S. Carlson, G. Daniel, P. Svedlindh, G. A. Seisenbaeva and V. G. Kessler, *RSC Adv*., 2014,4, 22606-22612
54. D. Ramirez, R. Vera, H. Gomez and C. Conajahua, J. *Chil. Chem. Soc*., 2005, 50 ,489-494.
55. X. Shi, T.A. Nguyen, Z. Suo, Y. Liu and R. Avci, *Surf. Coat. Techno*l.,2009, 204, 237–245.
56. S.K. Dhoke and A. Khanna, *Mater. Chem. Phys*., 2009, 117, 550–556.
57. J.R. Scully, *J. Electrochem.Soc*.,1989, 136, 979–990.
58. U. Rammelt and G. Reinhard, *Prog. Org. Coat*. ,1992, 21, 205–226.
59. G.W. Walter, Corrosion ,1991,32, 1059–1084.
60. A. Yabuki and K. Okumura, *Corros. Sci.* 2012, 59, 258–262.

Graphical abstract